NOLTA, IEICE

Paper

Nonlinear dynamics of a model of acoustic metamaterials with local resonators

Naoki Higashiyama [1], *Yusuke Doi* [2a)], *and Akihiro Nakatani* [2]

[1] *TOA Corporation*
7-2-1, Minatojimanaka-machi, Chuo-ku, Kobe, Hyogo, Japan

[2] *Department of Adaptive Machine Systems, Graduate School of Engineering Osaka University*
2-1 Yamadaoka, Suita, Osaka 565-0871, Japan

[a)] *doi@ams.eng.osaka-u.ac.jp*

Received July 12, 2016; Revised November 10, 2016; Published April 1, 2017

Abstract: Nonlinear dynamics of a model of acoustic metamaterials with local resonators are investigated numerically and theoretically. We focus on dynamics of band edge modes (BEMs) and zone boundary modes (ZBMs) which are on the upper bounds of acoustic bands and optical bands of the phonon dispersion band. It is found that, in a region of weak anharmonicity, higher harmonics of a fundamental mode and static displacement are excited in both BEM and ZBM if the geometrical relation between the main lattice and the local resonators has even-order nonlinearity. Numerical solutions of nonlinear periodic orbits which are continued from vibrations in the small amplitude limit by the shooting method indicate that structure of the periodic orbits of the local resonators depends on the form of nonlinear terms of the geometrical relation. Moreover, the nonlinear periodic orbits become unstable when the amplitude of the periodic orbit becomes larger. Direct numerical simulations show that unstable dynamics occur due to modulational instability. After destabilization of the nonlinear periodic orbits, spatial energy localization is also observed.

Key Words: nonlinear vibration, stability, energy localization

1. Introduction

Recently, metamaterials have been of great interest in various fields of engineering and science [1, 2]. The metamaterial is an artificial material with fine discrete structures in which functional elements are incorporated.

Metamaterials have firstly attracted in electromagnetic engineering. Veselago has predicted the existence of materials with negative permittivity and magnetic permeability [3]. Pendry has shown the possibility of a perfect lens based on the materials with the negative permittivity and magnetic permeability [4]. A practical artificial periodic structure which realizes the negative permittivity and

Nonlinear Theory and Its Applications, IEICE, vol. 8, no. 2, pp. 129–145 DOI: 10.1587/nolta.8.129

magnetic permeability has been proposed by Smith *et al.* [5]. Since these milestones, various studies on the electromagnetic metamaterial has been performed [6, 7].

An acoustic metamaterial can be regarded as an analogy of electromagnetic metamaterial [8, 9]. The acoustic metamaterials can be used to deal with elastic waves instead of electromagnetic waves by a periodic structure with the larger scale than that of the electromagnetic metamaterial. By designing and manufacturing various functional periodic structures, negative effective bulk modulus [10–12], negative effective mass density [13–16] can be realized. Moreover, acoustic metamaterials with both negative effective bulk modulus and negative effective mass density have been proposed theoretically and experimentally [17–21]. Using the negative effective bulk modulus and the negative effective mass density, various pioneering and important applications such as acoustic cloaking [22–32], acoustic superlens and hyperlens [33–42], and acoustic black hole devices [43, 44] have been proposed.

It has been pointed out that the local resonator is one of the key factors for realizing the negative effective elastic modulus. Liu *et al.* has made a sonic crystal with localized resonant structures [45]. In the theoretical study, it has been shown that the effective elastic modulus of the sonic crystal becomes negative [46]. In general, the local resonators are connected to the oscillators in the main lattice. The local resonators interact only with the main lattice. The geometric relation between the main lattice and the local resonators, which dominates the way of interaction between the main lattice and the local resonators, can be described by a certain geometric function. The geometric connection intrinsically has nonlinearity since it has the complex geometry. The nonlinearity due to the geometry can be dominant in vibration if the amplitude of vibration is large. In this sense, we can construct a mechanical model of the acoustic metamaterials as a nonlinear lattice model.

By introducing the nonlinearity to the mechanical model, a variety of complex dynamics such as excitation of higher harmonics, instability, and energy localized structure arises in the system. In this direction, various investigations on nonlinear acoustic metamaterials have been reported [47–55]. For the future development of nonlinear acoustic metamaterials, it is important to construct a mechanical model for nonlinear acoustic metamaterials and to deeply investigate basic dynamical properties of the mechanical model.

One of the expected dynamics in the nonlinear acoustic metamaterials is energy localization called discrete breathers (DBs) or intrinsic localized modes (ILMs) [56]. DBs are vibration modes with a higher frequency out of dispersion band of linear phonon modes. DBs are excited due to discreteness and nonlinearity of the system. Various studies have been performed theoretically and experimentally [57–59]. Considering nonlinear vibrations such as DBs, we can find much wider applications of metamaterials such as energy transportation, and local activation of functional elements. For this purpose, it is required to construct the method for exciting the DBs in the system. The most popular mechanism for the excitation of DBs is modulational instability of particular phonon modes. For theoretical lattices such as Fermi-Pasta-Ulam β (FPU-β) systems, nonlinear energy localization called chaotic breathers is excited from the modulational instability [60]. Therefore, it is important to investigate dynamics and stability of phonon modes of the acoustic metamaterials for future investigation of DBs in the acoustic metamaterials.

In this study, we construct a one-dimensional nonlinear lattice model for the acoustic metamaterials with inter-site local resonators. By using the constructed model, the effect of nonlinearity of geometric relation between the main lattice and the local resonators on the dynamics of the nonlinear lattice model is investigated.

The present paper is organized as follows. In section 2, the one-dimensional nonlinear lattice model is introduced. The linear dispersion relation of the system is discussed in section 3. In section 4, the dynamics of the lattice model in the region of weak nonlinearity is investigated by the perturbation analysis. Numerical results of the temporal evolution of the system in the linear approximation, weak nonlinearity, and strong nonlinearity are presented in section 5. The nonlinear periodic orbit obtained by the shooting method is discussed in Section 6. Finally, conclusions are given in section 7.

2. Model

We consider a one-dimensional lattice model which represents acoustic metamaterials with local resonators. The schematic description of the model is shown in Fig. 1. The Hamiltonian of the system is given as follows:

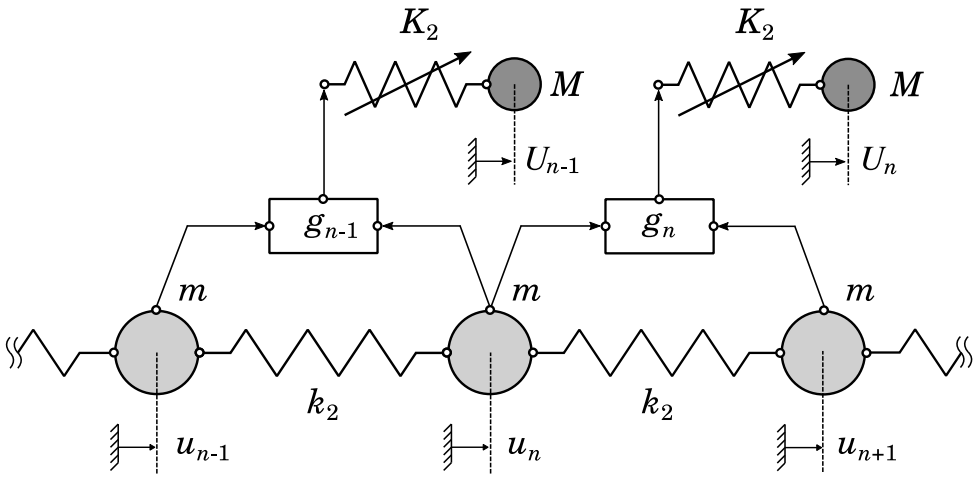

Fig. 1. Model.

$$H = \sum_{n=1}^{N} \left[\frac{1}{2} m \dot{u}_n^2 + \frac{1}{2} M \dot{U}_n^2 + v_n + V_n \right], \tag{1}$$

where u_n is the displacement of the nth particle in the main lattice, U_n is the displacement of the nth local resonator, m and M are the mass of the particle in the main lattice and the local resonators, respectively. The interaction between neighboring particles in the main lattice is v_n and the interaction between the nth local resonator and the nth and $(n+1)$th particles in the main lattice is V_n:

$$v_n = \frac{1}{2} k_2 (u_{n+1} - u_n)^2 \tag{2}$$

$$V_n = \frac{1}{2} K_2 (U_n - g_n(\mathbf{u}))^2, \tag{3}$$

where k_2 represents the strength of the linear interaction between the particles in the main lattice, K_2 represents the strength of interaction between the local resonators and the main lattice. We consider the periodic boundary condition.

The equilibrium position of the nth local resonator is determined by the position of particles in the main lattice, which are connected to the nth local resonator. We introduce a function g_n in terms of $\mathbf{u} = (u_1, u_2, \cdots, u_N)$ which describes the geometric relation between the local resonators and the connecting particles in the main lattice.

From Eq. (1), the equations of motion for the particles in the main lattice and the local resonators are

$$m \ddot{u}_n - k_2 (u_{n+1} - 2u_n + u_{n-1}) - \sum_l K_2 (U_l - g_l(\mathbf{u})) \frac{\partial g_l(\mathbf{u})}{\partial u_n} = 0, \tag{4}$$

$$M \ddot{U}_n + K_2 (U_n - g_n(\mathbf{u})) = 0. \tag{5}$$

Hereafter, we introduce some constants shown in Table I. We assume that $\omega_0^{\text{main}} = 1$ without loss of the generality.

Next, we assume that the nth local resonator is connected to the nth and $(n+1)$th particles in the

Table I. Definition of constants.

Definition	Description
$\theta = M/m$	Mass ratio
$\delta = K_2/k_2$	Spring constant ratio of K_2 to k_2
$\omega_0^{\mathrm{main}} = \sqrt{k_2/m}$	Eigenfrequency of the main lattice
$\omega_0^{\mathrm{lr}} = \sqrt{K_2/m}$	Eigenfrequency of the local resonators

main lattice. Therefore, the function $g_n(\mathbf{u})$ can be described in terms of u_n and u_{n+1}. Considering the nonlinear effect due to the geometry of system, $g_n(u_n, u_{n+1})$ becomes the following form:

$$g_n = \beta_1(u_{n+1} - u_n) + \beta_2(u_{n+1} - u_n)^2 + \beta_3(u_{n+1} - u_n)^3, \tag{6}$$

where β_1 is the harmonic coefficient, β_2 is the asymmetric anharmonic coefficient, β_3 is the symmetric anharmonic coefficient. Asymmetric anharmonicity usually appears due to the geometrical constraint of the system. The symmetric anharmonicity is introduced in order to investigate nonlinear interaction, i.e., FPU β lattices.

Substituting Eq. (6) into Eq. (4) and (5), and ignoring the higher than 4th order terms, we obtain the equations of motion as follows:

$$\begin{aligned}
\ddot{u}_n = &\left(1 + \delta\beta_1^2\right)\left\{(u_{n+1} - u_n) - (u_n - u_{n-1})\right\} - \delta\beta_1^2\left(U_n - U_{n-1}\right) \\
&+3\delta\beta_1\beta_2\left\{(u_{n+1} - u_n)^2 - (u_n - u_{n-1})^2\right\} \\
&-2\delta\beta_2\left\{U_n(u_{n+1} - u_n) - U_{n-1}(u_n - u_{n-1})\right\} \\
&+\delta\left(4\beta_1\beta_3 + 2\beta_2^2\right)\left\{(u_{n+1} - u_n)^3 - (u_n - u_{n-1})^3\right\} \\
&-3\delta\beta_3\left\{U_n(u_{n+1} - u_n)^2 - U_{n-1}(u_n - u_{n-1})^2\right\},
\end{aligned} \tag{7}$$

$$\ddot{U}_n = \frac{\delta}{\theta}\left\{-U_n + \beta_1(u_{n+1} - u_n) + \beta_2(u_{n+1} - u_n)^2 + \beta_3(u_{n+1} - u_n)^3\right\}. \tag{8}$$

3. Linear dispersion relation

By neglecting the higher order terms in Eq. (7) and Eq. (8), we obtain the linearized equations of motion:

$$\ddot{u}_n = (1 + \delta\beta_1^2)(u_{n+1} - 2u_n + u_{n-1}) - \delta\beta_1^2(U_n - U_{n-1}), \tag{9}$$

$$\ddot{U}_n = \frac{\delta}{\theta}\left[-U_n + \beta_1(u_{n+1} - u_n)\right]. \tag{10}$$

Substituting a plane wave form with a wave number κ and an angular frequency ω

$$u_n = \frac{1}{2}\left[C_1 e^{i(n\kappa - \omega t)} + C_1^* e^{-i(n\kappa - \omega t)}\right], \tag{11}$$

$$U_n = \frac{1}{2}\left[C_2 e^{i(n\kappa - \omega t)} + C_2^* e^{-i(n\kappa - \omega t)}\right], \tag{12}$$

into Eq. (9)–(10) and some calculations, we obtain the dispersion relation

$$\omega^4 - \left[\frac{\delta}{\theta} + 2(1 + \delta\beta_1^2)(1 - \cos\kappa)\right]\omega^2 + \frac{2\delta}{\theta}(1 - \cos\kappa) = 0, \tag{13}$$

where C_1 and C_2 are complex constants and $*$ indicates complex conjugate.

Figure 2 shows the dispersion curve with $\beta_1 = 1$, $\delta = 1$ and $\theta = 1$. It is found that two branches are formed in the dispersion curve, i.e., the acoustic branch and the optical branch. The forbidden bands appear above the optical band and between the acoustic band and optical band which is shown as the gray regions in Fig. 2. Nonlinear vibration modes including DBs [58] can be excited in these forbidden bands. The range of frequency of the forbidden band is characterized by zone boundary

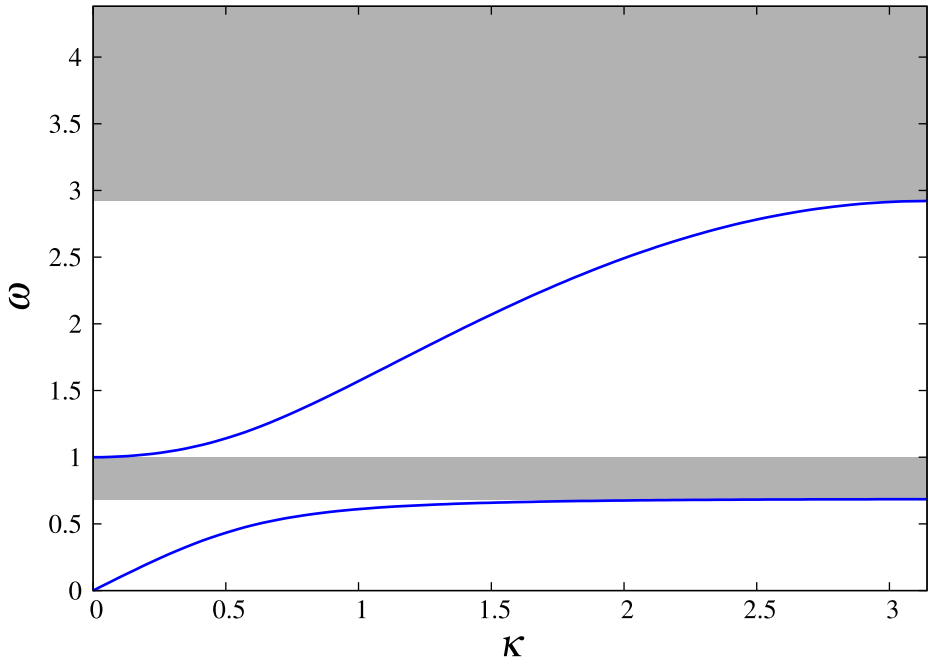

Fig. 2. Dispersion relation of the system. The parameters are $\beta_1 = 1$, $\delta = 1$ and $\theta = 1$.

mode (ZBM) and band edge mode (BEM) which are the normal modes with the maximum frequency in the optic band and acoustic band, respectively. The angular frequencies of ZBM and BEM are

$$\omega_{\mathrm{ZBM}} = \frac{\sqrt{2}}{2}\sqrt{\frac{\delta}{\theta} + 4(1+\delta\beta_1^2) + \sqrt{\left[\frac{\delta}{\theta} + 4(1+\delta\beta_1^2)\right]^2 - \frac{16\delta}{\theta}}} \tag{14}$$

$$\omega_{\mathrm{BEM}} = \frac{\sqrt{2}}{2}\sqrt{\frac{\delta}{\theta} + 4(1+\delta\beta_1^2) - \sqrt{\left[\frac{\delta}{\theta} + 4(1+\delta\beta_1^2)\right]^2 - \frac{16\delta}{\theta}}}. \tag{15}$$

It is known that the dynamics and stability of the ZBM are important for understanding nonlinear dynamics of the discrete systems since the instability can lead to exciting the nonlinear coherent structure such as nonlinear normal mode and DBs. We investigate the behavior of the ZBM and the BEM with large amplitude in the next section.

4. Perturbation analysis of ZBM and BEM in weak nonlinearity

In nonlinear lattices, normal modes are affected by the nonlinearity of system. One of the most significant effects is the appearance of instability. Unstable dynamics leads to spatial modulation of the homogeneous vibration. It is well known that the modulational instability of the ZBEs and BEMs excites energy localization called discrete breathers. Therefore, we are interested in the behavior of ZBM and BEM which leads to the excitation of energy localization.

In order to investigate the behavior of the vibration in weak nonlinear region of the system, we perform the perturbation analysis of the equation of motion (7) and (8) by expanding u_n and U_n:

$$u_n = u_n^{(0)} + \varepsilon u_n^{(1)} + O(\varepsilon^2), \tag{16}$$

$$U_n = U_n^{(0)} + \varepsilon U_n^{(1)} + O(\varepsilon^2), \tag{17}$$

where ε is a small constant.

Substituting (16) and (17) into (7) and (8), and collecting terms in terms of ε, we obtain the following equations at the leading order:

$$\frac{d^2u_n^{(0)}}{dt^2} = \left(1+\delta\beta_1^2\right)\left(u_{n+1}^{(0)} - 2u_n^{(0)} + u_{n-1}^{(0)}\right) - \delta\beta_1\left(U_n^{(0)} - U_{n-1}^{(0)}\right), \tag{18}$$

$$\frac{d^2U_n^{(0)}}{dt^2} = \frac{\delta}{\theta}\left\{-U_n^{(0)} + \beta_1\left(u_{n+1}^{(0)} - u_n^{(0)}\right)\right\}. \tag{19}$$

This is just a linearized version of the equation of motion (9)–(10). Therefore, the solutions of the leading order are given as:

$$u_n^{(0)} = \frac{1}{2}\left\{\bar{C}_1 e^{i(n\kappa_1-\omega_1 t)} + \bar{C}_1^* e^{-i(n\kappa_1-\omega_1 t)}\right\}, \tag{20}$$

$$U_n^{(0)} = \frac{1}{2}\left\{\frac{\beta_1\left(\delta/\theta\right)\left(1-e^{i\kappa_1}\right)}{\omega_1^2-\delta/\theta}\bar{C}_1 e^{i(n\kappa_1-\omega_1 t)} + \frac{\beta_1\left(\delta/\theta\right)\left(1-e^{-i\kappa_1}\right)}{\omega_1^2-\delta/\theta}\bar{C}_1^* e^{-i(n\kappa_1-\omega_1 t)}\right\}, \tag{21}$$

where $\bar{C}_1$ and $\bar{C}_1^*$ are complex constants, ω_1 and κ_1 satisfy the dispersion relation (13).

In the next order ε, we obtain equations as

$$\begin{aligned}\frac{d^2u_n^{(1)}}{dt^2} = &\left(1+\delta\beta_1^2\right)\left(u_{n+1}^{(1)} - 2u_n^{(1)} + u_{n-1}^{(1)}\right) - \delta\beta_1\left(U_n^{(1)} - U_{n-1}^{(1)}\right)\\ &+3\delta\beta_1\beta_2\left\{\left(u_{n+1}^{(0)} - u_n^{(0)}\right)^2 - \left(u_n^{(0)} - u_{n-1}^{(0)}\right)^2\right\}\\ &-2\delta\beta_2\left\{U_n^{(0)}\left(u_{n+1}^{(0)} - u_n^{(0)}\right) - U_{n-1}^{(0)}\left(u_n^{(0)} - u_{n-1}^{(0)}\right)\right\}\end{aligned} \tag{22}$$

$$\frac{d^2U_n^{(1)}}{dt^2} = \frac{\delta}{\theta}\left\{-U_n^{(1)} + \beta_1\left(u_{n+1}^{(1)} - u_n^{(1)}\right)\right\} + \frac{\delta}{\theta}\beta_2\left(u_{n+1}^{(0)} - u_n^{(0)}\right)^2. \tag{23}$$

Substituting the solutions of the leading order (20) and (21) into (22) and (23), we obtain

$$\begin{aligned}\frac{d^2u_n^{(1)}}{dt^2} = &\left(1+\delta\beta_1^2\right)\left(u_{n+1}^{(1)} - 2u_n^{(1)} + u_{n-1}^{(1)}\right) - \delta\beta_1\left(U_n^{(1)} - U_{n-1}^{(1)}\right)\\ &-i\delta\beta_1\beta_2\frac{3\omega_1^2-\delta/\theta}{\omega_1^2-\delta/\theta}\sin\kappa_1(1-\cos\kappa_1)\bar{C}_1^2 e^{2i(n\kappa_1-\omega_1 t)}\\ &+i\delta\beta_1\beta_2\frac{3\omega_1^2-\delta/\theta}{\omega_1^2-\delta/\theta}\sin\kappa_1(1-\cos\kappa_1)\bar{C}_1^{*2} e^{-2i(n\kappa_1-\omega_1 t)},\end{aligned} \tag{24}$$

$$\begin{aligned}\frac{d^2U_n^{(1)}}{dt^2} = &\frac{\delta}{\theta}\left\{-U_n^{(1)} + \beta_1\left(u_{n+1}^{(1)} - u_n^{(1)}\right)\right\}\\ &+\frac{1}{4}\frac{\delta}{\theta}\beta_2\left(1-e^{i\kappa_1}\right)^2\bar{C}_1^2 e^{2i(n\kappa_1-\omega_1 t)} + \frac{1}{4}\frac{\delta}{\theta}\beta_2\left(1-e^{-i\kappa_1}\right)^2\bar{C}_1^{*2} e^{-2i(n\kappa_1-\omega_1 t)}\\ &+\frac{\delta}{\theta}\beta_2(1-\cos\kappa_1)|\bar{C}_1|^2.\end{aligned} \tag{25}$$

By substituting $\kappa_1 = \pi$ into (24) and (25), we obtain the equations for ZBM and BEM as follows,

$$\frac{d^2u_n^{(1)}}{dt^2} = \left(1+\delta\beta_1^2\right)\left(u_{n+1}^{(1)} - 2u_n^{(1)} + u_{n-1}^{(1)}\right) - \delta\beta_1\left(U_n^{(1)} - U_{n-1}^{(1)}\right), \tag{26}$$

$$\begin{aligned}\frac{d^2U_n^{(1)}}{dt^2} = &\frac{\delta}{\theta}\left\{-U_n^{(1)} + \beta_1\left(u_{n+1}^{(1)} - u_n^{(1)}\right)\right\} + \frac{\delta}{\theta}\beta_2\bar{C}_1^2 e^{-2i\omega_1 t} + \frac{\delta}{\theta}\beta_2\bar{C}_1^{*2} e^{2i\omega_1 t}\\ &+2\frac{\delta}{\theta}\beta_2|\bar{C}_1|^2.\end{aligned} \tag{27}$$

It is found that the homogeneous part of Eq. (26) and (27) is the same form as the equation at the leading order (18) and (19). Therefore, the homogeneous solution of Eq. (26) and (27) are given as

$$u_n^{(h)} = \frac{1}{2}\left[C_3 e^{i(n\kappa_2-\omega_2 t)} + C_3^* e^{-i(n\kappa_2-\omega_2 t)}\right], \tag{28}$$

$$U_n^{(h)} = \frac{1}{2}\left[C_4 e^{i(n\kappa_2-\omega_2 t)} + C_4^* e^{-i(n\kappa_2-\omega_2 t)}\right], \tag{29}$$

which are the same form as Eq. (20) and (21). The parameters C_3, C_3^*, C_4, and C_4^* are complex constants. The wavenumber κ_2 and angular frequency ω_2 satisfy the relation (13).

When $\beta_2 = 0$, the inhomogeneous terms in Eq. (27) vanish. This means that the homogeneous solutions (28) and (29) are just the solutions. Moreover, if we set the initial condition as $u_n^{(1)}(0) = U_n^{(1)}(0) = 0$, any excitation does not arise.

When $\beta_2 \neq 0$, we have to consider the particular solution of Eq. (26) and (27) since the inhomogeneous terms in Eq. (27) do not vanish. In terms of $u_n^{(1)}$, we can set the particular solution $u_n^{(p)} = 0$. In terms of $U_n^{(1)}$, the particular solution is $U_n^{(p)}(t) = b\exp(-2i\omega_1 t) + b^* \exp(2i\omega_1 t) + C$, since the inhomogeneous terms have the frequency $2\omega_1$ and do not depend on n in Eq. (27). Substituting this into Eq. (27) and solving in terms of the constants b, b^* and C, we obtain

$$U_n^{(p)}(t) = -\frac{\delta/\theta}{4\omega_1^2 - \delta/\theta}\beta_2 \bar{C}_1^2 \exp(-2i\omega_1 t) + 2\beta_2 \left|\bar{C}_1\right|^2 - \frac{\delta/\theta}{4\omega_1^2 - \delta/\theta}\beta_2 \bar{C}_1^{*2} \exp(2i\omega_1 t). \tag{30}$$

We can choose $C_3 = 0$ which corresponds to the initial conditions $\Delta u_n(0) = 0$ in terms of the homogeneous solutions. In this case, the homogeneous Eq. (27) becomes

$$\frac{d^2 U_n^{(1)}}{dt^2} = -\frac{\delta}{\theta} U_n^{(1)}. \tag{31}$$

Therefore, the homogeneous solution for ΔU_n solved as

$$U_n^{(h)}(t) = \frac{1}{2}\left(B\exp(-i\sqrt{\delta/\theta}t) + B^* \exp(i\sqrt{\delta/\theta}t)\right), \tag{32}$$

where B and B^* are complex constants. Combining the homogeneous solution and the particular solution with the initial condition $U_n^{(1)}(0) = 0$, we obtain

$$\begin{aligned} U_n^{(1)} = {} & \beta_2\left(\frac{\delta/\theta}{4\omega_1^2 - \delta/\theta}\bar{C}_1^2 - |\bar{C}_1|^2\right) e^{-i\sqrt{\delta/\theta}t} + \beta_2\left(\frac{\delta/\theta}{4\omega_1^2 - \delta/\theta}\bar{C}_1^{*2} - |\bar{C}_1|^2\right) e^{i\sqrt{\delta/\theta}t} \\ & -\beta_2 \frac{\delta/\theta}{4\omega_1^2 - \delta/\theta}\bar{C}_1^2 e^{-2i\omega_1 t} - \beta_2 \frac{\delta/\theta}{4\omega_1^2 - \delta/\theta}\bar{C}_1^{*2} e^{2i\omega_1 t} + 2\beta_2\left|\bar{C}_1\right|^2. \end{aligned} \tag{33}$$

Equation (33) indicates that, in the case that $\beta_2 \neq 0$, the vibration due the particular term is excited in the local resonator even if we set $\Delta U_n(0) = 0$. The frequencies of the perturbation of the local resonator are the natural frequency of the local resonator and the second harmonics of the ZBM or BEM. Moreover, the local resonators have static displacement $2\beta_2\left|\bar{C}_1\right|^2$.

Substituting (21) and (33) into (17), it is found that the local resonators have frequencies of the ZBM (14) or BEM (15), and the natural frequency $\sqrt{\delta/\theta}$. In general, the ratio of these frequencies is an irrational number. Therefore, the vibrations of the local resonator become the quasi-periodic orbit.

5. Temporal evolution of ZBM and BEM

In this section, we investigate the temporal evolution of the ZBM and BEM of Eq. (7) and (8).

Initial displacement of particles of the ZBM and BEM is

$$\begin{aligned} u_n(0) &= (-1)^n A, \\ U_n(0) &= (-1)^n \frac{2\beta_1 \frac{\delta}{\theta}}{\omega^2 - \frac{\delta}{\theta}} A, \end{aligned} \tag{34}$$

where we set $\delta = \theta = 1$ and $\beta_1 = 1$, A is the amplitude of the ZBM and BEM, ω is the angular frequency of the ZBM and BEM, respectively. Initial velocity of the particles is $\dot{u}_n(0) = \dot{U}_n(0) = 0$. The ZBM and BEM are excited to the system by taking the initial displacement (34) with the angular frequency $\omega = \omega_{\mathrm{ZBM}}$ (14) and ω_{BEM} (15), respectively. In the present case, we can set $\omega_{\mathrm{ZBM}} = 2.92$ and $\omega_{\mathrm{BEM}} = 0.685$.

The numerical integration of the equation of motion (7) and (8) is performed by the 4th order Runge-Kutta method. A time step of the numerical integration is $\Delta t = 0.0001$.

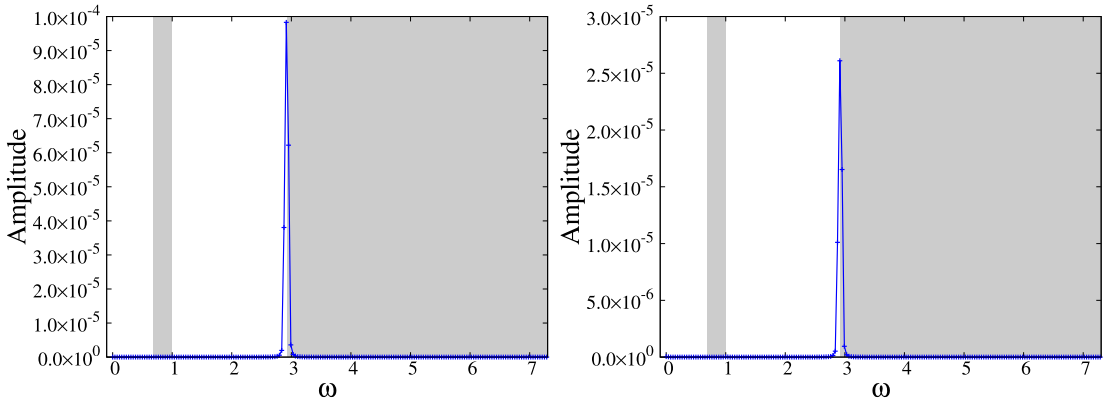

Fig. 3. Spectrum of vibration from initial conditions of ZBM with $A = 0.0001$ for $\beta_1 = \beta_2 = \beta_3 = 1$: (Left)main lattice and (Right)local resonator.

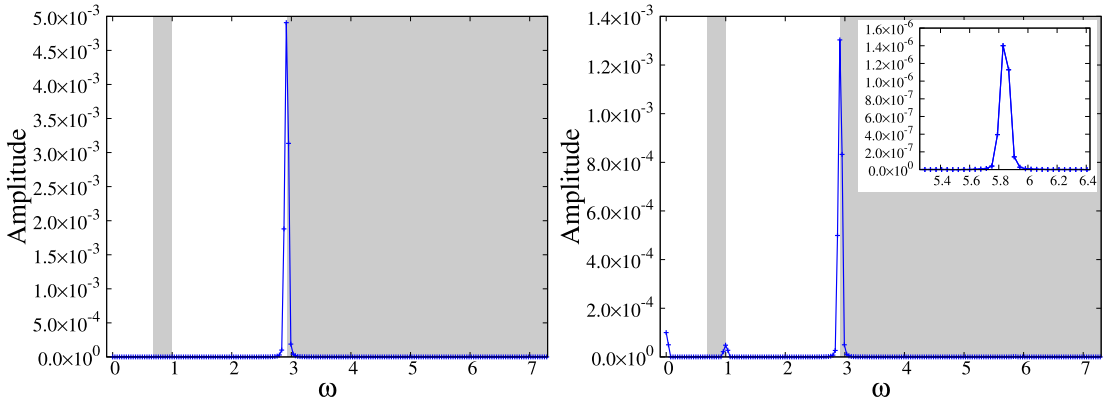

Fig. 4. Spectrum of vibration from initial conditions of ZBM with $A = 0.005$ for $\beta_1 = \beta_2 = \beta_3 = 1$: (Left)main lattice and (Right)local resonator.

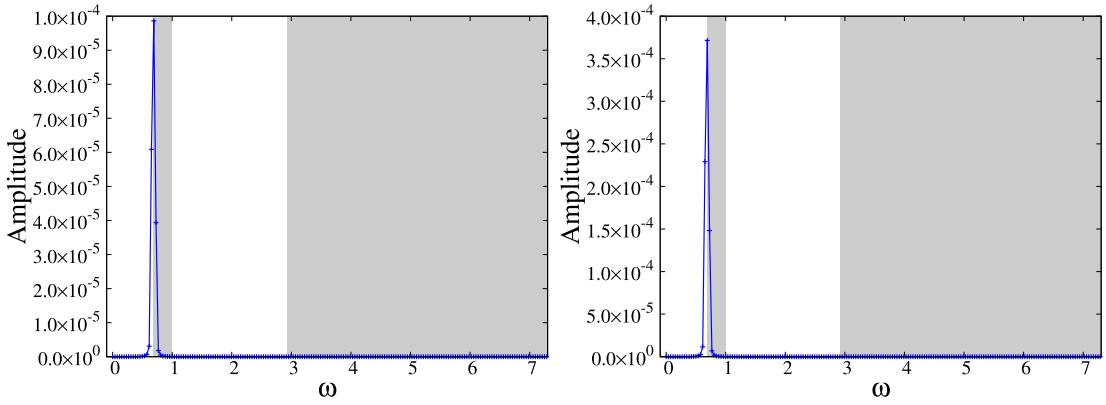

Fig. 5. Spectrum of vibration from initial conditions of BEM with $A = 0.0001$ for $\beta_1 = \beta_2 = \beta_3 = 1$: (Left)main lattice and (Right)local resonator.

Figure 3 shows the temporal spectrum of ZBM with $A = 0.0001$ for $\beta_1 = 1, \beta_2 = 1$ and $\beta_3 = 1$. The gray bands represent the forbidden bands of the system. A single peak at the upper bound of the optic branch is observed both in the main lattice and the local resonators. This peak corresponds to the fundamental frequency $\omega = 2.92$. It is found that the initial amplitude $A = 0.0001$ is so small that the vibration can be regarded as the linear vibration.

In the case that $A = 0.005$ as shown in Fig. 4, a single peak is observed in the main lattice. However, several new peaks are observed at $\omega = 1.0 = \sqrt{\delta/\theta}$ and $\omega = 5.89 = 2\omega_{\mathrm{ZBM}}$ in the local resonators. This is because the nonlinear interaction between the local resonator and the main lattice becomes significant. These frequencies correspond to the vibration which is described by Eq. (33).

Figures 5 and 6 show the spectrum of BEM with $A = 0.0001$ and $A = 0.005$, respectively. Effect of

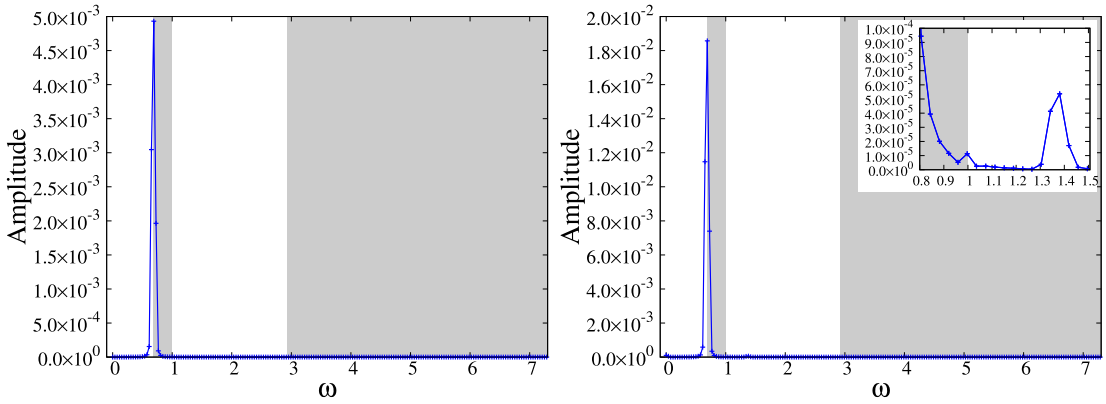

Fig. 6. Spectrum of vibration from initial conditions of BEM with $A = 0.005$ for $\beta_1 = \beta_2 = \beta_3 = 1$: (Left)main lattice and (Right)local resonator.

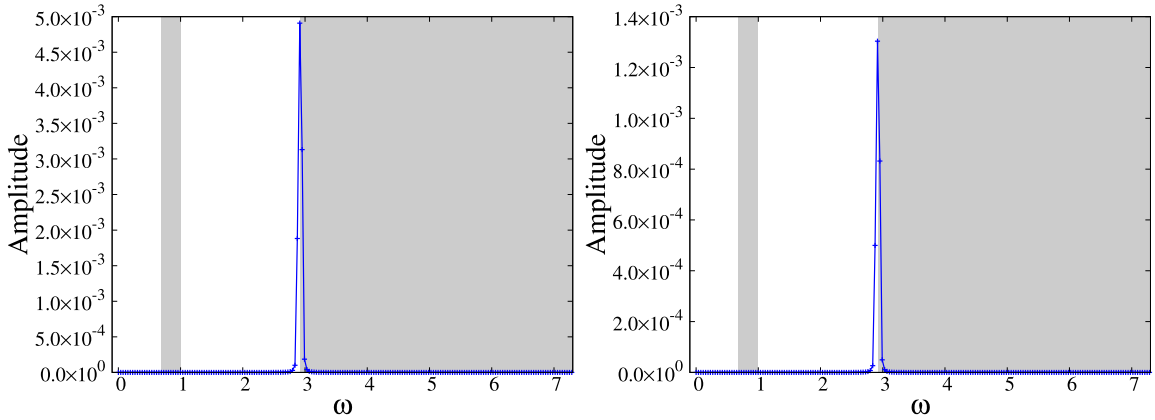

Fig. 7. Spectrum of vibration from initial conditions of ZBM with $A = 0.005$ for $\beta_1 = 1$,$\beta_2 = 0$, and $\beta_3 = 1$: (Left)main lattice and (Right)local resonator.

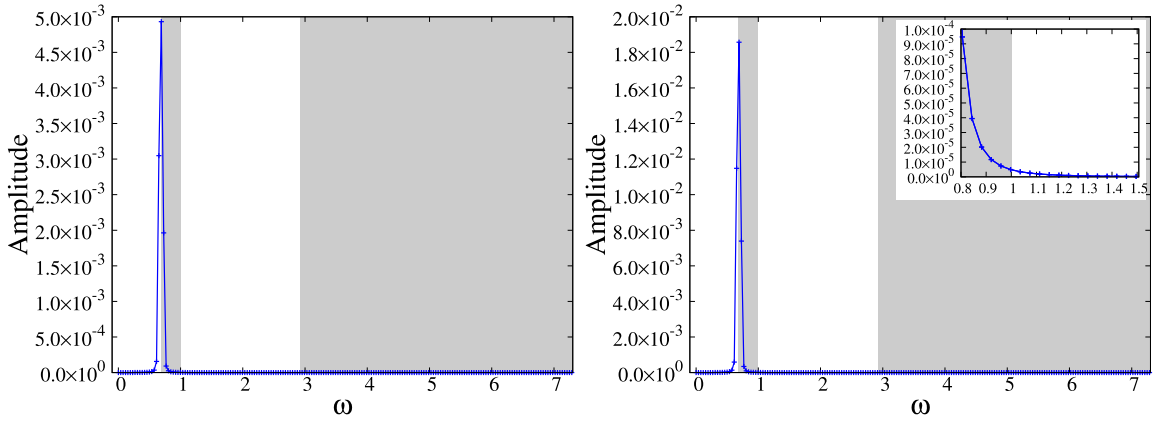

Fig. 8. Spectrum of vibration from initial conditions of BEM with $A = 0.005$ for $\beta_1 = 1$, $\beta_2 = 0$, and $\beta_3 = 1$: (Left)main lattice and (Right)local resonator.

the nonlinearity of the interaction between the local resonator and the main lattice becomes significant as the peaks at $\omega = 1.0 = \sqrt{\delta/\theta}$ and $\omega = 1.37 = 2\omega_{\mathrm{BEM}}$ in the spectrum of the local resonator in Fig. 6. These peaks of the spectrum can be also explained by Eq. (33).

Figure 7 and 8 show the spectrum of vibration of ZBM and BEM for $\beta_1 = 1, \beta_2 = 0$ and $\beta_3 = 1$. Unlike the case of $\beta_2 \neq 0$ shown in Fig. 4 and Fig. 6, only a single peak which corresponds to ω_{ZBM} or ω_{BEM} is observed in the local resonators. Therefore, no perturbation which has the frequency, $\sqrt{\delta/\theta}$ or $2\omega_{\mathrm{ZBM,BEM}}$ is excited. This result is consistent with the discussion in Section 4.

We also investigate the temporal evolution of the system in the large anharmonic case which can not be able to investigate by the perturbation analysis discussed in Section 4. Figure 9 shows the

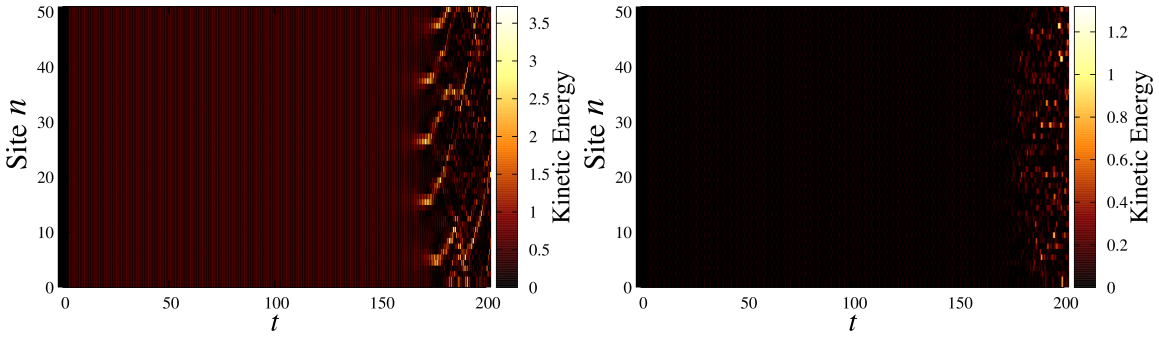

Fig. 9. Temporal evolution of distribution of kinetic energy of particles in ZBM with $A = 0.31$ for $\beta_1 = 1, \beta_2 = 1$, and $\beta_3 = 1$: (Left)main lattice and (Right)local resonator. The horizontal axis indicates time and the vertical axis indicates site number n of particles.

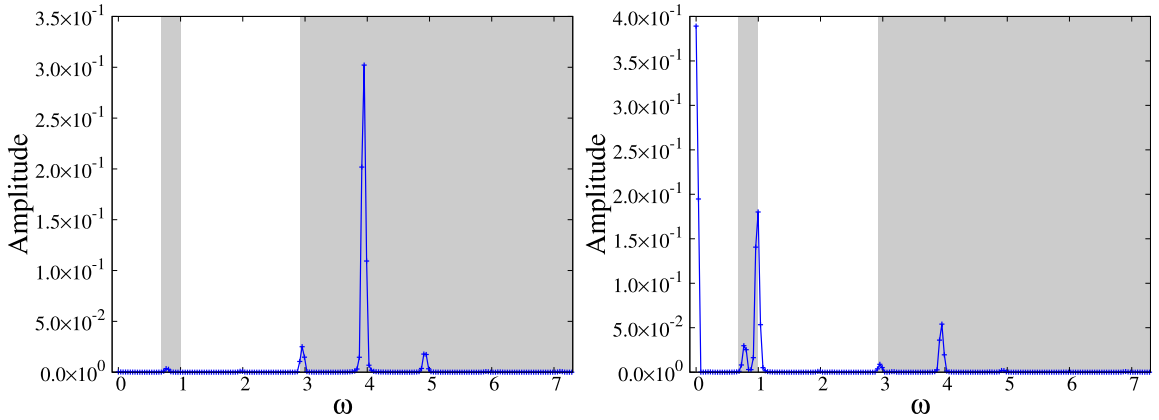

Fig. 10. Spectrum of vibration from initial conditions of ZBM with $A = 0.31$ for $\beta_1 = 1, \beta_2 = 1$, and $\beta_3 = 1$: (Left)main lattice and (Right)local resonator.

distribution of kinetic energy of particles in the ZBM for $A = 0.31$, $\beta_1 = 1$, $\beta_2 = 1$ and $\beta_3 = 1$. The energy localization due to the modulational instability of ZBM can be observed at $t = 163$ in the main lattice. Then, non-uniform energy distribution arises in both the main lattice and the local resonators. Figure 10 shows the spectrum of vibration before $t = 163$. In the main lattice, the largest peak is at $\omega = 3.96$ and two side peaks are at $\omega = 2.96$ and $\omega = 4.88$. These peaks are in the forbidden bands. In the local resonators, the larger peaks are at $\omega = 1$ in the lower forbidden band and at $\omega = 4.88$ in the higher forbidden band, and side peaks are at $\omega = 0.769$ in the lower band and at $\omega = 3.96$ in the higher forbidden band. We also find the largest peak at $\omega = 0$ in the local resonators.

In hard (positive) nonlinearity of the system, the frequency of vibration can increas as the amplitude of the vibration increases. Therefore, in the case of much larger amplitude with $A = 0.31$ than the linear approximation, the large (positive) shift of elementary frequency is observed from $\omega_{\mathrm{ZBM}} = 2.92$ to $\omega = 3.96$ in the main lattice. Several side peaks are observed both in the main lattice and the local resonators. This can be regarded as the excitation of modulational instability of the ZBM in which envelope is modulated with longer wavelength.

Figure 11 shows the distribution of kinetic energy of particles in the ZBM for $A = 0.31$, $\beta_1 = 1$, $\beta_2 = 0$ and $\beta_3 = 1$. In the main lattice, the spatial energy localized structures are excited at $t = 50$. The localized structures wanders in the system with keeping their structure. This is like chaotic breathers which are observed in wide class of nonlinear discrete systems [60]. Figure 12 shows the spectrum before the excitation of the localized structure. The frequency shift of ZBM is also observed in the case of Fig. 10 as observed in Fig. 12.

It is concluded that, in the large anharmonic case, the unstable dynamics due to the modulational instability arises in both cases that $\beta_2 = 0$ and $\beta_2 \neq 0$. Moreover, the spatial energy localized structures are excited after unstable dynamics arises. In the case that $\beta_2 = 0$, chaotic breather is observed. This fact indicates that the present system can support the excitation of DBs [58].

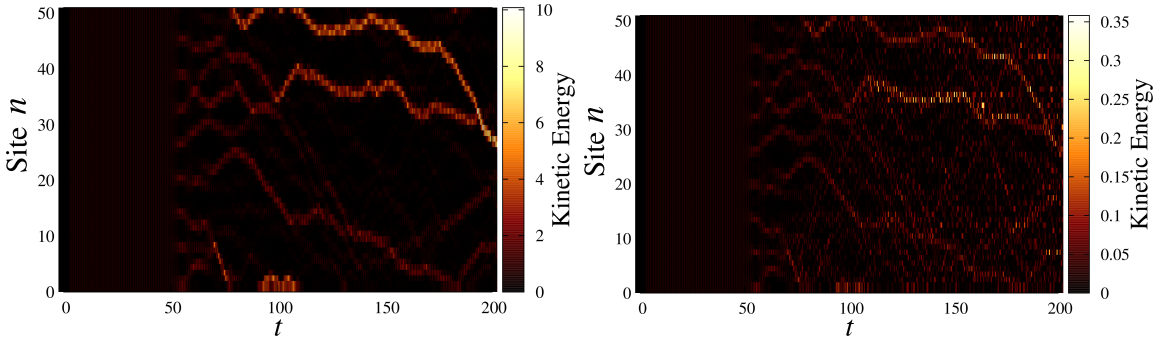

Fig. 11. Temporal evolution of distribution of kinetic energy of particles in ZBM with $A = 0.31$ for $\beta_1 = 1, \beta_2 = 0$, and $\beta_3 = 1$: (Left)main lattice and (Right)local resonator. The horizontal axis indicates time and the vertical axis indicates site number n of particles.

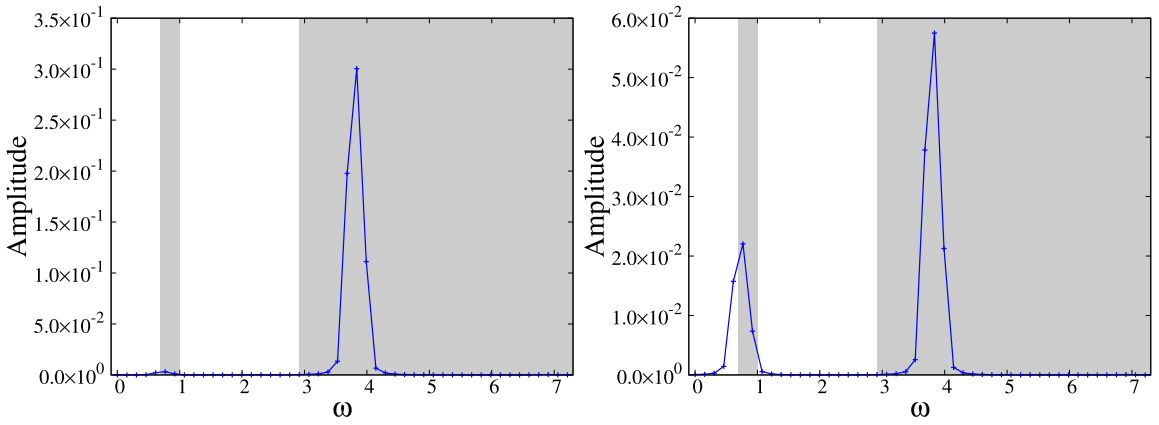

Fig. 12. Spectrum of vibration from initial conditions of ZBM with $A = 0.31$ for $\beta_1 = 1, \beta_2 = 0$, and $\beta_3 = 1$: (Left)main lattice and (Right)local resonator.

6. Nonlinear periodic solution from ZBM

In order to investigate the dependence of frequency and stability on the amplitude of vibration, we search the nonlinear periodic orbits which are continued from the vibration modes in the small amplitude limit by the shooting method. Moreover, we investigate linear stability of the numerical solution of periodic orbits.

Let $\tilde{u}_n(t)$ and $\tilde{U}_n(t)$ be numerical solutions of the periodic orbit with a period of T and $\Delta u_n(t)$ and $\Delta U_n(t)$ be small deviation from the periodic orbit. Substituting $u_n(t) = \tilde{u}_n(t) + \Delta u_n(t)$ and $U_n(t) = \tilde{U}_n(t) + \Delta U_n(t)$ into Eq. (7)–(8) and subtracting equations of motion with $u_n(t) = \tilde{u}_n(t)$ and $U_n(t) = \tilde{U}_n(t)$, we obtain equation for $\Delta u_n(t)$) and $\Delta U_n(t)$:

$$
\begin{aligned}
\Delta\ddot{u}_n = &\left(1+\delta\beta_1^2\right)\left\{(\Delta u_{n+1}-\Delta u_n)-(\Delta u_n-\Delta u_{n-1})\right\}-\delta\beta_1^2\left(\Delta U_n-\Delta U_{n-1}\right)\\
&+6\delta\beta_1\beta_2\left\{(\tilde{u}_{n+1}-\tilde{u}_n)(\Delta u_{n+1}-\Delta u_n)-(\tilde{u}_n-\tilde{u}_{n-1})(\Delta u_n-\Delta u_{n-1})\right\}\\
&-2\delta\beta_2\left\{\tilde{U}_n(\Delta u_{n+1}-\Delta u_n)+(\tilde{u}_{n+1}-\tilde{u}_n)\Delta U_n-\tilde{U}_{n-1}(\Delta u_n-\Delta u_{n-1})-(\tilde{u}_n-\tilde{u}_{n-1})\Delta U_{n-1}\right\}\\
&+6\delta\left(2\beta_1\beta_3+\beta_2^2\right)\left\{(\tilde{u}_{n+1}-\tilde{u}_n)^2(\Delta u_{n+1}-\Delta u_n)-(\tilde{u}_n-\tilde{u}_{n-1})^2(\Delta u_n-\Delta u_{n-1})\right\}\\
&-3\delta\beta_3\left\{(\tilde{u}_{n+1}-\tilde{u}_n)^2\Delta U_n-(\tilde{u}_n-\tilde{u}_{n-1})^2\Delta U_{n-1}+2\tilde{U}_n(\tilde{u}_{n+1}-\tilde{u}_n)(\Delta u_{n+1}-\Delta u_n)\right.\\
&\left.-2\tilde{U}_{n-1}(\tilde{u}_n-\tilde{u}_{n-1})(\Delta u_n-\Delta u_{n-1})\right\},
\end{aligned}
\tag{35}
$$

$$
\begin{aligned}
\Delta\ddot{U}_n = &\frac{\delta}{\theta}\left\{-\Delta U_n+\beta_1(\Delta u_{n+1}-\Delta u_n)+2\beta_2(\tilde{u}_{n+1}-\tilde{u}_n)(\Delta u_{n+1}-\Delta u_n)\right.\\
&\left.+3\beta_3(\tilde{u}_{n+1}-\tilde{u}_n)^2(\Delta u_{n+1}-\Delta u_n)\right\}.
\end{aligned}
\tag{36}
$$

Let $\mathbf{X} = \{u_n, U_n, \dot{u}_n, \dot{U}_n\}$ be the state variable. The variational Eqs. (35) and (36) is rewritten to

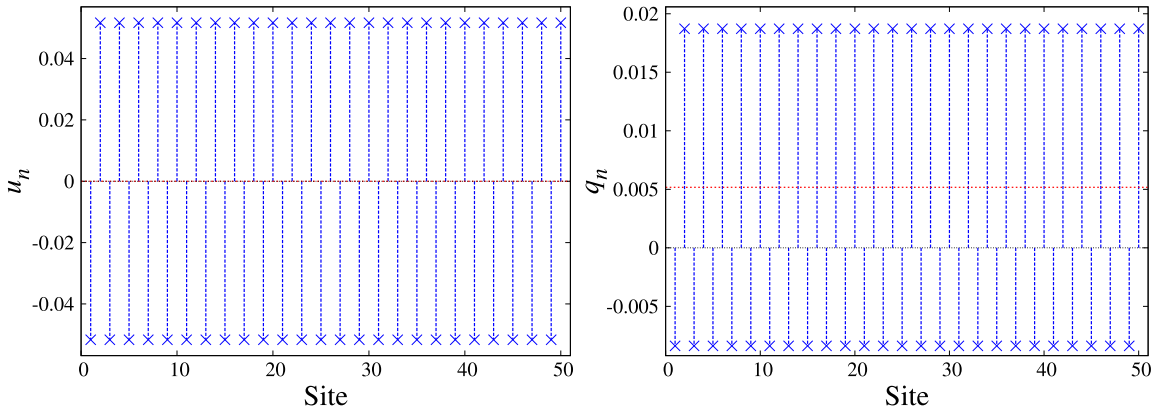

Fig. 13. Displacement of ZBM with $\omega = 2.9475$: (Left)main lattice and (Right)local resonator for $\beta_1 = 1$, $\beta_2 = 1$ and $\beta_3 = 1$.

$$\Delta\dot{\mathbf{X}} = \frac{\partial \mathbf{F}}{\partial \mathbf{X}} \Delta\mathbf{X}, \tag{37}$$

where $\mathbf{F}$ indicates $\{\dot{u}_n, \dot{U}_n, \text{RHS of Eq. (7)}, \text{RHS of Eq. (8)}\}$. Since $\partial\mathbf{F}/\partial\mathbf{X}$ consists of $\tilde{u}_n$ and $\tilde{U}_n$, $\partial\mathbf{F}/\partial\mathbf{X}$ is T-periodic. In this case, there exists a regular matrix $\mathbf{M}(T)$ such that

$$\mathbf{X}(t+T) = \mathbf{M}(T)\mathbf{X}(t). \tag{38}$$

The matrix $\mathbf{M}(t)$ is called monodromy matrix. Let σ be eigenvalues of $\mathbf{M}(t)$. The periodic orbit is unstable if an eigenvalue is outside the unit circle in the complex plane. In Hamilton systems, if σ is an eigenvalue of the monodromy matrix, $1/\sigma$ is also an eigenvalue. Therefore, the periodic orbit is stable if and only if all eigenvalues are on the unit circle in the complex plane.

Figure 13 shows the displacement of the nonlinear periodic solution from the ZBM with $\omega = 2.9475$ in the system for $\beta_1 = 1$, $\beta_2 = 1$, and $\beta_3 = 1$. The displacement of the main lattice is the same form as in the linear vibration

$$u_n = (-1)^n A' \cos\omega t, \tag{39}$$

where A' is a real constant. The local resonators, on the other hand, has a constant displacement:

$$U_n = (-1)^n B' \cos\omega t + C', \tag{40}$$

where B' and C' are real constants.

Figure 14(a) shows the relation between the amplitude of the main lattice A' and the angular frequency ω. The angular frequency increases as the amplitude increases. Figure 14(b) indicates the relation between the amplitude of the main lattice A' and the amplitude of the local resonators B'. The amplitude of the local resonator also increases as the amplitude of the main lattice increases. However, the derivative dB'/dA' gradually decreases. The static displacement C' and its derivative dC'/dA' increase as the amplitude A' increases. As to the local resonators, the static displacement becomes dominant as the amplitude of the main system becomes larger.

We calculate the eigenvalues of the monodromy matrix which give the growth rates of variation from the periodic orbit. The periodic orbit is unstable if one of the eigenvalues is greater than 1 since the present system is the Hamiltonian system. Figure 14(d) shows the relation between the eigenvalues $|\sigma|$ and the amplitude A'. It is found that the eigenvalue greater than 1 appears at $A' = 0.0178$. Therefore, the periodic orbit from ZBM becomes unstable when the amplitude $A' \geq 0.0178$.

In the case that $\beta_2 = 0$, it is found that the angular frequency ω and the amplitude of the local resonators B' increase as the amplitude of the main system A' increases as shown in Figs. 15(a) and (b). However, the static displacement C' vanishes.

Figure 15(c) indicates the eigenvalues of the monodromy matrix. All eigenvalues are one up to $A' = 0.0177$ which is almost same as the case that $\beta_2 = 1$.

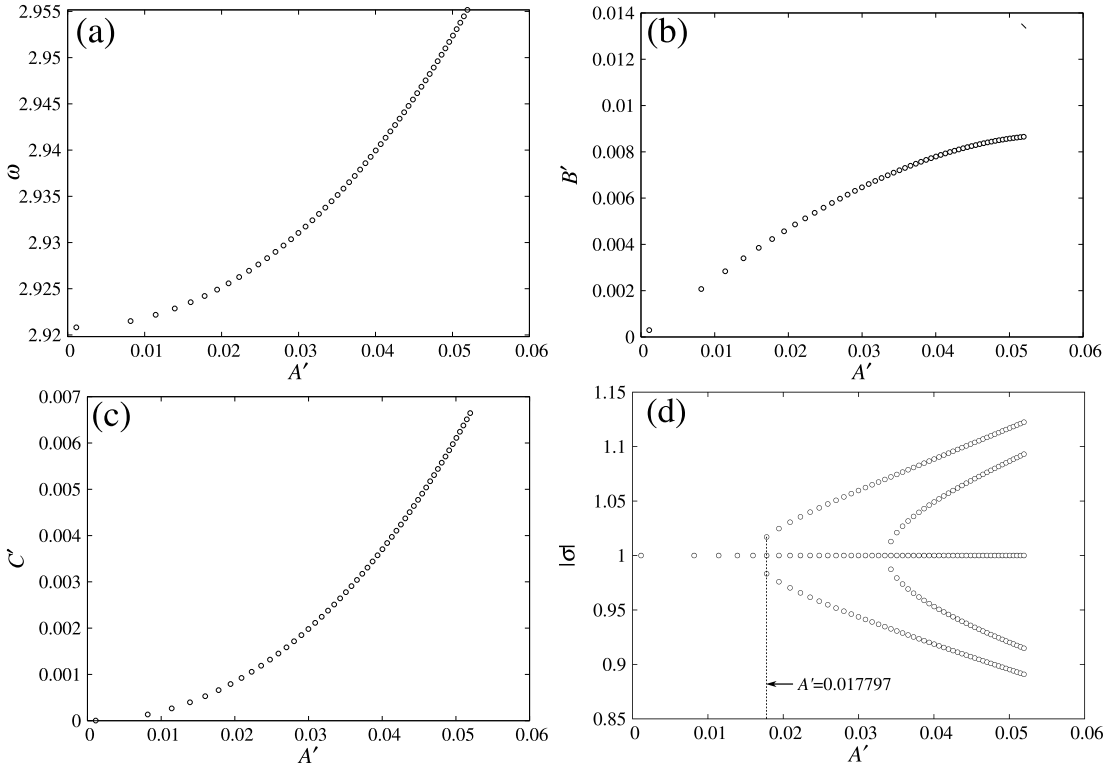

Fig. 14. Amplitude A' dependence on the periodic orbit from ZBM for $\beta_1 = 1$, $\beta_2 = 1$ and $\beta_3 = 1$: (a)angular frequency, (b)amplitude of local resonator, (c)static displacement of the local resonator, and (d)eigenvalues of the monodoromy matrix.

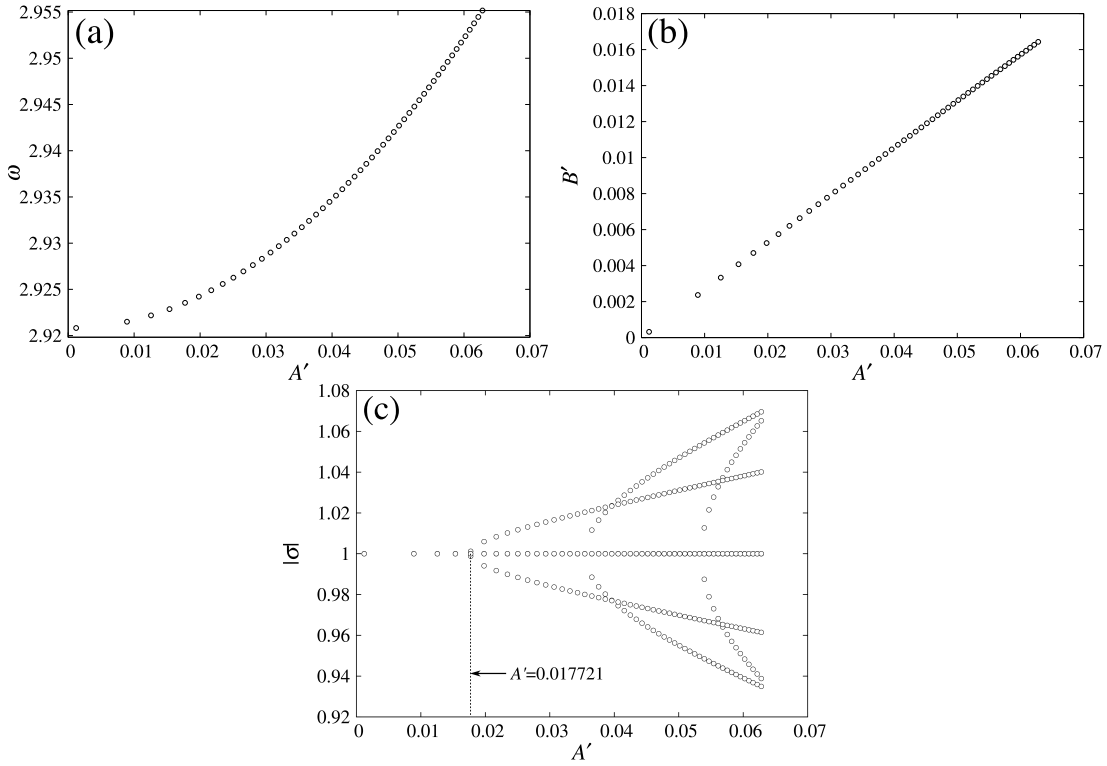

Fig. 15. Amplitude A' dependence on the periodic orbit from ZBM for $\beta_1 = 1$, $\beta_2 = 0$ and $\beta_3 = 1$: (a)angular frequency, (b)amplitude of the local resonator, and (c)eigenvalues of the monodoromy matrix.

In summary, the structure of nonlinear periodic orbit which are continued from ZBM depends on the parameter β_2. In case that $\beta_2 \neq 0$, the static displacement arises in the local resonators. In case that $\beta_2 = 0$, the static displacement vanishes. This result is consistent with the temporal evolution of ZBM with large amplitude discussed in Section 5. The linear stability of the nonlinear periodic orbits is almost same in both cases.

7. Conclusions

In this paper, we investigate the nonlinear dynamics of the mechanical model of the acoustic metamaterials with the local resonators. In our model, the geometric relation between the main lattice and the local resonators is described by the nonlinear function g_n. Due to the local resonators, the phonon band is divided into the acoustic band and the optic band. Therefore, two upper bounds of the phonon band or ZBM and BEM exist in the system.

The dynamics of ZBM and BEM in the region of weak nonlinearity is investigated by the direct numerical integration of the equation of motion and perturbation analysis. When the function g_n has the even-order nonlinearity, the vibrations with the second harmonics of the main frequency and the natural frequency of the local resonator is excited. Moreover, the stationary displacement is excited.

The numerical solutions of the nonlinear periodic orbit which are continued from the ZBM in the small amplitude limit are calculated by the shooting method. The static displacement of the local resonator arises when the function g_n has the even-order nonlinearity. The nonlinear periodic orbit becomes unstable when the amplitude of the main lattice reaches to the particular value.

The dynamics of ZBM and BEM beyond the region of weak nonlinearity is investigated by the numerical integration of the equation of motion with the initial condition of large amplitude. The initial displacement becomes unstable due to the modulational instability regardless of the existence of the even-order terms in the function g_n. After destabilization of the initial displacement, the spatial energy localized structure are excited. This fact implies that the present system supports the existence of DB.

Acknowledgments

The second author (Y.D.) was partially supported by a Grant-in-Aid for Scientific Research (C), No. 16K05041 from Japan Society for the Promotion of Science (JSPS).

References

[1] M. Kadic, T. Bückmann, R. Schittny, and M. Wegener, "Metamaterials beyond electromagnetism," *Reports on Progress in Physics*, vol. 76, no. 12, 126501, November 2013.

[2] J. Christensen, M. Kadic, O. Kraft, and M. Wegener, "Vibrant times for mechanical metamaterials," *MRS Communications*, vol. 5, no. 3, pp. 453–462, July 2015.

[3] V.G. Veselago, "The electrodynamics of substances with simultaneously negative values of ϵ and μ," *Physics-Uspekhi*, vol. 10, no. 4, pp. 509–514, January 1968.

[4] J.B. Pendry, A.J. Holden, D.J. Robbins, and W.J. Stewart, "Magnetism from conductors and enhanced nonlinear phenomena," *IEEE Transactions on Microwave Theory and Techniques*, vol. 47, no. 11, pp. 2075–2084, November 1999.

[5] D.R. Smith, W.J. Padilla, D.C. Vier, S.C. Nemat-Nasser, and S. Schultz, "Composite medium with simultaneously negative permeability and permittivity," *Phys. Rev. Lett.*, vol. 84, no. 18, 4184, May 2000.

[6] J.B. Pendry, "Negative refraction makes a perfect lens," *Phys. Rev. Lett.*, vol. 85, no. 18, 3966, October 2000.

[7] J.B. Pendry, D. Schurig, and D.R. Smith, "Controlling electromagnetic fields," *Science*, vol. 312, no. 5781, pp. 1780–1782, June 2006.

[8] L. Fok, M. Ambati, and X. Zhang, "Acoustic metamaterials," *MRS Bulletin*, vol. 33, pp. 931–934, October 2008.

[9] G. Ma and P. Sheng, "Acoustic metamaterials: From local resonances to broad horizons," *Science Advances*, vol. 2, no. 2, e1501595, February 2016.

[10] Z.Y. Liu, X. Zhang, Y. Mao, Y.Y. Zhu, Z. Yang, C.T. Chan, and P. Sheng, "Locally resonant sonic materials," *Science*, vol. 289, no. 5485, pp. 1734–1736, September 2000.
[11] N. Fang, D. Xi, J. Xu, M. Ambati, W. Srituravanich, C. Sun, and X. Zhang, "Ultrasonic metamaterials with negative modulus," *Nat. Mater.*, vol. 5, no. 6, pp. 452–456, April 2006.
[12] S.H. Lee, C.M. Park, Y.M. Seo, Z.G. Wang, and C.K. Kim, "Acoustic metamaterial with negative modulus," *J. Phys. Condens. Matter.*, vol. 21, no. 17, 175704, March 2009.
[13] S. Yao, X. Zhou, and G. Hu, "Experimental study on negative effective mass in a 1D mass-spring system," *New J. Phys.*, vol. 10, 043020, April 2008.
[14] Z. Yang, J. Mei, M. Yang, N.H. Chan, and P. Sheng, "Membrane-type acoustic metamaterial with negative dynamic mass," *Phys. Rev. Lett.*, vol. 101, 204301, November 2008.
[15] H.H. Huang, C.T. Sun, and G.L. Huang, "On the negative effective mass density in acoustic metamaterials," *International Journal of Engineering Science*, vol. 47, no. 4, pp. 610–617, April 2009.
[16] S.H. Lee, C.M. Park, Y.M. Seo, Z.G. Wang, and C.K. Kim, "Acoustic metamaterial with negative density," *Phys. Lett. A*, vol. 373, no. 48, pp. 4464–4469, December 2009.
[17] J. Li and C.T. Chan, "Double negative acoustic metamaterial," *Phys. Rev. E*, vol. 70, no. 5, 055602, November 2004.
[18] Y. Ding, Z. Liu, C. Qiu, and J. Shi, "Metamaterial with simultaneously negative bulk modulus and mass density," *Phys. Rev. Lett.*, vol. 99, no. 9, 093904, August 2007.
[19] S.H. Lee, C.M. Park, Y.M. Seo, Z.G. Wang, and C.K. Kim, "Composite acoustic medium with simultaneously negative density and modulus," *Phys. Rev. Lett.*, vol. 104, 054301, February 2010.
[20] L. Fok and X. Zhang, "Negative acoustic index metamaterial," *Phys. Rev. B*, vol. 83, no. 21, 214304, June 2011.
[21] N. Kaina, F. Lemoult, M. Fink, and G. Lerosey, "Negative refractive index and acoustic superlens from multiple scattering in single negative metamaterials," *Nature*, vol. 525, pp. 77–81, September 2015.
[22] G.W. Milton, M. Briane, and J.R. Willis, "On cloaking for elasticity and physical equations with a transformation invariant form," *New J. Phys.*, vol. 8, 248, October 2006.
[23] S.A. Cummer and D. Schurig, "One path to acoustic cloaking," *New J. Phys.*, vol. 9, 45, March 2007.
[24] H. Chen and C.T. Chan, "Acoustic cloaking in three dimensions using acoustic metamaterials," *Appl. Phys. Lett.*, vol. 91, 183518, November 2007.
[25] H. Chen and C.T. Chan, "Acoustic cloaking in three dimensions using acoustic metamaterials," *Appl. Phys. Lett.*, vol. 91, no. 18, 183518, November 2007.
[26] S.A. Cummer, B.I. Popa, D. Schurig, D.R. Smith, J.B. Pendry, M. Rahm, and A. Starr, "Scattering theory derivation of a 3D acoustic cloaking shell," *Phys. Rev. Lett.*, vol. 100, 024301, January 2008.
[27] Y. Cheng, F. Yang, J.Y. Xu, and X.J. Liu, "A multilayer structured acoustic cloak with homogeneous isotropic materials," *Appl. Phys. Lett.*, vol. 92, no. 15, 151913, April 2008.
[28] D. Torrent and J. Sánchez-Dehesa, "Acoustic cloaking in two dimensions: A feasible approach," *New J. Phys.*, vol. 10, 063015, June 2008.
[29] J. Hu, X. Zhou, and G. Hu, "A numerical method for designing acoustic cloak with arbitrary shapes," *Computational Materials Science*, vol. 46, no. 3, pp. 708–712, September 2009.
[30] S. Zhang, C. Xia, and N. Fang, "Broadband Acoustic Cloak for Ultrasound Waves," *Phys. Rev. Lett.*, vol. 106, no. 2, 024301, January 2011.
[31] N. Stenger, M. Wilhelm, and M. Wegener, "Experiments on elastic cloaking in thin plates," *Phys. Rev. Lett.*, vol. 108, 014301, January 2012.
[32] J. Zhu, T. Chen, Q. Liang, X. Wang, J. Xiong, and P. Jiang, "A unidirectional acoustic cloak for multilayered background media with homogeneous metamaterials," *J. Phys. D: Appl. Phys.*, vol. 48, no. 30, 305502, July 2015.
[33] M. Ambati, N. Fang, C. Sun, and X. Zhang, "Surface resonant states and superlensing in

acoustic metamaterials," *Phys. Rev. B*, vol. 75, no. 19, 195447, May 2007.
[34] Z. Liu, S. Durant, H. Lee, Y. Pikus, N. Fang, Y. Xiong, C. Sun, and X. Zhang, "Far-field optical superlens," *Nano Lett.*, vol. 7, pp. 403–408, January 2007.
[35] M.H. Lu, C. Zhang, L. Feng, J. Zhao, Y.F. Chen, Y.W. Mao, J. Zi, Y.Y. Zhu, S.N. Zhu, and N.B. Ming, "Superlenses to overcome the diffraction limit," *Nat. Mater.*, vol. 6, pp. 744–748, June 2007.
[36] X. Zhang and Z. Liu, "Superlenses to overcome the diffraction limit," *Nat. Mater.*, vol. 7, pp. 435–441, June 2008.
[37] J. Li, L. Fok, X. Yin, G. Bartal, and X. Zhang, "Experimental demonstration of an acoustic magnifying hyperlens," *Nat. Mater.*, vol. 8, no. 12, pp. 931–934, October 2009.
[38] S. Zhang, L. Yin, and N. Fang, "Focusing ultrasound with an acoustic metamaterial network," *Phys. Rev. Lett.*, vol. 102, 194301, May 2009.
[39] J. Li, L. Fok, X. Yin, G. Bartal, and X. Zhang, "Experimental demonstration of an acoustic magnifying hyperlens," *Nat. Mater.*, vol. 8, pp. 931–934, October 2009.
[40] Y. Lai, Y. Wu, P. Sheng, and Z.Q. Zhang, "Hybrid elastic solids," *Nat. Mater.*, vol. 10, pp. 620–624, June 2011.
[41] J. Christensen and F.J. García de Abajo, "Anisotropic metamaterials for full control of acoustic waves," *Phys. Rev. Lett.*, vol. 108, 124301, March 2012.
[42] Z. Liang, T. Feng, S. Lok, F. Liu, K.B. Ng, C.H. Chan, and J. Wang, "Reflected wavefront manipulation based on ultrathin planar acoustic metasurfaces," *Sci. Rep.*, vol. 3, 1614, August 2013.
[43] A. Climente, D. Torrent, and J.S. Dehesa, "Omnidirectional broadband acoustic absorber based on metamaterials," *Appl. Phys. Lett.*, vol. 100, 144103, April 2012.
[44] J. Song, P. Bai, Z. Hang, and Y. Lai, "Acoustic coherent perfect absorbers," *New. J. Phys.*, vol. 16, 033026, March 2014.
[45] Z. Liu, X. Zhang, Y, Mao, Y.Y. Zhu, Z. Yang, C.T. Chan, and P. Sheng, "Locally resonant sonic materials," *Science*, vol. 289, no. 5485, pp. 1734–1736, September 2000.
[46] Z. Liu, C.T. Chan, and P. Sheng, "Analytic model of phononic crystals with local resonances," *Phys. Rev. B*, vol. 71, no. 1, 014103, January 2005.
[47] J. Lydon, M. Serra-Garcia, and C. Daraio, "Local to extended transitions of resonant defect modes," *Phys. Rev. Lett.*, vol. 113, 185503, October 2014.
[48] P. Wang, F. Casadei, S. Shan, J.C. Weaver, and K. Bertoldi, "Harnessing buckling to design tunable locally resonant acoustic metamaterials," *Phys. Rev. Lett.*, vol. 113, 014301, July 2014.
[49] B. Florijn, C. Coulais, and M. van Hecke, "Programmable mechanical metamaterials," *Phys. Rev. Lett.*, vol. 113, 175503, October 2014.
[50] A. Spadoni and C. Daraio, "Generation and control of sound bullets with a nonlinear acoustic lens," *Proc. Natl. Acad. Sci. U.S.A.*, vol. 107, pp. 7230–7234, April 2010.
[51] F. Li, P. Anzel, J. Yang, P.G. Kevrekidis, and C. Daraio, "Granular acoustic switches and logic elements," *Nat. Commun.*, vol. 5, 5311, October 2014.
[52] B.-I. Popa and S.A. Cummer, "Non-reciprocal and highly nonlinear active acoustic metamaterials," *Nat. Commun.*, vol. 5, 3398, February 2014.
[53] B. Liang, X.S. Guo, J. Tu, D. Zhang, and J.C. Cheng, "An acoustic rectifier," *Nat. Mater.*, vol. 9, pp. 989–992 October 2010.
[54] B. Liang, B. Yuan, and J.-C. Cheng, "Acoustic diode: Rectification of acoustic energy flux in one-dimensional systems," *Phys. Rev. Lett.*, vol. 103, 104301, September 2009.
[55] N. Boechler, G. Theocharis, and C. Daraio, "Bifurcation-based acoustic switching and rectification," *Nat. Mater.*, vol. 10, pp. 665–668, July 2011.
[56] A.J. Sievers and S. Takeno, "Intrinsic localized modes in anharmonic crystals," *Phys. Rev. Lett.*, vol. 61, pp. 970–973, August 1988.
[57] S. Flach and A.V. Gorbach, "Discrete breathers—Advances in theory and applications," *Phys. Rep.*, vol. 467, 1, May 2008.
[58] K. Yoshimura, Y. Doi, and M. Kimura, "Localized modes in nonlinear discrete systems," in

Progress in Nanophotonics III, eds. M. Ohtsu and T. Yatsui, pp. 119–166, Springer, New York, 2014.

[59] S.V. Dmitriev, "Discrete breathers in crystals: Energy localization and transport," Journal of Micromechanics and Molecular Physics, vol. 1, 1630001, July 2016.

[60] T. Cretegny, T. Dauxois, S. Ruffo, and A. Torcini, "Localization and equipartition of energy in the β-FPU chain: Chaotic breathers," in *Physica D*, vol. 121, no. 1–2, pp. 109–126, October 1998.